

ANGULER DISTRIBUTIONS OF BEAM LOSS PROTONS AT J-PARC LINAC*

Hiroyuki Sako, Tomofumi Maruta, Akihiko Miura, J-PARC Center, Japan Atomic Energy Agency,
Japan

Abstract

In J-PARC linac, at ACS (Annular-Coupled Structure linac) section, highest beam loss was observed. This beam loss is considered to be caused mainly by H^0 generated by ionization of H^- by residual gas in the beam duct. The H^0 is further changed to H^+ when penetrating the beam duct. We have developed a detector system consisting of 8 planes of scintillating fiber hodoscopes. Each hodoscope consists of 16 fibers of $4 \times 4 \text{ mm}^2$ square or 4 mm diameter circle cross sections with 64 mm length. The upstream detector (4 planes) is separated from the downstream detector (4 planes) by about 1.5 m to measure time-of-flight of charged particles. Each detector can move in horizontal and vertical directions with stepping motors. We have measured angular and energy distributions of the protons from Oct. 2012 to May 2013.

INTRODUCTION

We measure tracks of H^+ (protons) originated from the H^0 produced inside the beam duct at ACS11 section using the scintillating fiber hodoscope system. For detailed description of the detector system, refer to Ref. [1-4].

We measure energy of the protons with the time-of-flight between the upstream detector and the downstream detector. Each detector system consists of two fiber planes to measure horizontal positions and two planes to measure vertical planes. We define the plane from upstream to downstream as (H0, H1, V0, V1, H2, H3, V2, V3), where signals of V3 are not read out. The upstream and downstream detectors move independently in the horizontal and vertical directions.

We search for a straight track both in the x-z projection and in the y-z projection, where x is horizontal, y is vertical, and z is along the beam axis. We require hits in all the 7 planes (H0-H4 and V0-V3) and apply cuts in the residuals and χ^2 of the straight line fit of the track.

EXPERIMENT

We measured beam loss charged tracks from Dec. 2012 to May 2013. The upstream and downstream detectors are positioned at the beam height and horizontal positions were varied from 0 to 600 mm with respect to the beam center. In this analysis, we use data sets at the first medium bunch (first 100 nsec of the macro pulse).

Fig. 1 shows the spectrum of the time-of-flight between H1 and H2 (first and fourth) Planes. There is a peak of the proton signal (red curve) on rather large background

(green curve). The signal to background ration depends on the track angle to the beam axis, and ~ 1 at maximum. In order to extract the number of signal protons, we fit the spectrum with a combined formula with a Gaussian signal and a Lorentzian background. The fit result is shown as a red and a green curves in Fig. 1, and the signal is shown as a blue curve.

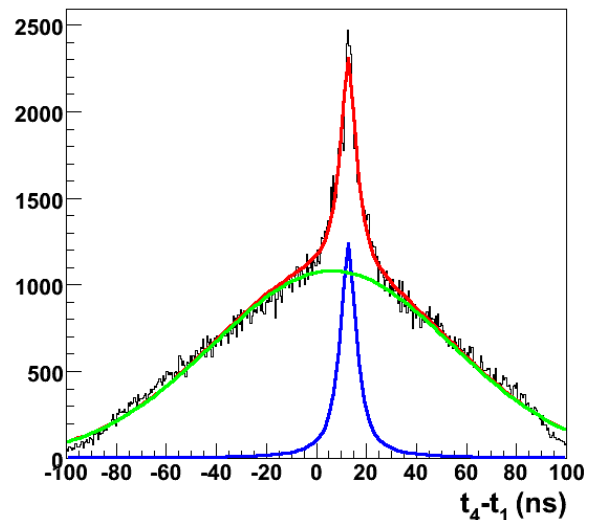


Figure 1: Time-of-flight spectrum (nsec) at $\theta_x=4.6$ deg.

RADIATION DAMAGE

We worry about radiation damages of the detector, since plastic scintillator used in our detector is weak against radiation.

Fig. 2 shows beam loss measured by a nearby beam loss proportional counter and peak beam current at the upstream MEBT1. There is a 30 mA peak in Apr. 14-21, 2013, while for other time periods, beam current is stable around 20-22 mA. After that event, from Apr. 29 to May 10, beam loss is $\sim 10\%$ higher than the other time periods.

The top figure of Fig. 3 shows the beam loss proton spatial density defined below as a function of the date in the whole experimental period. These three points are measured at the same geometrical conditions of the detectors. The loss density decreases by $\sim 40\%$ from the beginning to the end of the experiment. Since we suspected this may be due to radiation damages in the scintillating fibers, we compared the peak signal amplitude of the proton tracks in Plane H2 as shown in

*Work supported by JSPS KAKENHI Grant Numbers 23656063, 24510134.

#hiroyuki.sako@j-parc.jp

the bottom of Fig. 3. We observed almost no change in the amplitude from the beginning to Apr. 4, and then $\sim 15\%$ decreases in May 20. This may be due to radiation damage of 30 mA beams in Apr. 14-21 shown in the top of Fig. 2.

The measurements affected by the possible radiation damage after Apr. 21 are only in a limited data set, namely the data with the upstream detector position $x_u = 400$ mm.



Figure 2: Top: The beam loss pulse amplitude as a function of the date measured by a proportional counter at ACS11. Bottom: The peak beam current (mA) as a function of the date at the upstream of MEBT1.

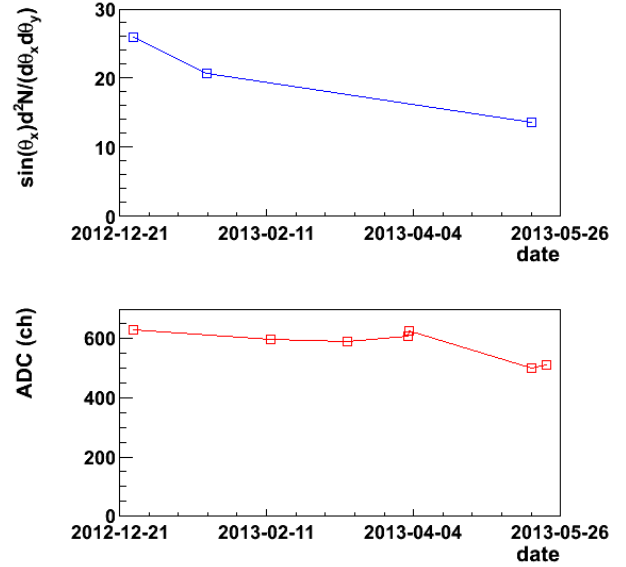


Figure 3: The beam loss spatial density ($\text{deg}^{-2}\text{m}^{-1}$) (top) and the signal amplitude (bottom) as a function of date.

RESULTS

Before showing the beam loss measurement results, we define the number of beam loss protons per macro pulse per unit length (m) along the beam axis as follows;

$$\frac{dN}{dz} = \int_{\theta_x=0}^{\pi/2} \int_{\theta_y=0}^{2\pi} \rho(\theta_x) d\theta_x d\theta_y,$$

where θ_x and θ_y are the horizontal and the vertical track angles with respect to the beam axis, and we define the proton spatial density as follows;

$$\rho(\theta_x) = \sin \theta_x \frac{d^3N}{d\theta_x d\theta_y dz}.$$

From the reconstructed number of proton tracks (N_{track}) within a data set (a run), we derive the number of protons per macro pulse (N) as the following formula;

$$N = \frac{N_{track} N_{coin}}{N_{macro} N_{trig}},$$

where N_{track} is the number of tracks within the data set, N_{macro} is the number of macro pulses (the number of events), N_{coin} is the number of triggers in the macro pulse within the data set, which are defined as coincidence signals between the dynode signals of the PMT for H0-H1 and the PMT for H2-H3, and N_{trig} is the number of triggers taken by the data acquisition system (DAQ). N_{trig} is equal to N_{macro} , since the DAQ can take only one trigger event per macro pulse, with the dead time of a few msec, while the repetition period of the macro pulse is 40 msec.

We set the horizontal position of the upstream detector at 100, 200, 300, 350, and 400 mm, and varied the horizontal position of the downstream detector from 0 to 600 mm, whereas we fixed the vertical detector positions at the beam height.

Fig. 4 shows the proton spatial density ($\text{deg}^{-2}\text{m}^{-1}$) as a function of θ_x , where we use FWHM of Gaussian fit functions (namely 2.35σ) for the ranges, $d\theta_x$, $d\theta_y$, and dz .

Symbols in different colors represent different upstream horizontal detector positions (x_u). The curves show Gaussian fits for each data set. The highest density of 52 observed at $x_u=300$ mm. Peaks are observed at $\theta_x \sim 6$ deg for $x_u=300$ and 350 mm, at $\theta_x \sim 7$ deg at $x_u=400$ mm, at ~ 8 deg at $x_u=100$ mm, and at ~ 11 deg at $x_u=200$ mm. In the simulation we observed peaks at ~ 5 deg, which may be consistent in case of $x_u=300-400$ mm.

Fig. 5 shows the same spatial densities but plotted as a function of the source z-position. The source z-position is defined as the track z-position at the closest approach of the track to the z-axis. The origin is defined as the middle position between the upstream and the downstream detectors, and the positive z means the downstream of the beam. At larger x_u we measure beam loss from more upstream positions, and combining all data set, the covered z-positions are 2–16 m downstream from the detector. Peaks are observed at ~ -3 m for $x_u=100$ mm, at ~ -2 m for $x_u=200$ mm, ~ -4.5 m for $x_u=300$ mm, ~ -5 m for $x_u=350$ mm, and ~ -5.5 m for $x_u=400$ mm.

By integrating over θ_x and θ_y , we can estimate the full solid angle proton numbers per macro pulse of 500 μsec per unit length (dN/dz) (1/m). In the x-direction, we integrate the Gaussian function in Fig. 4, while in the vertical direction we assume flat distributions in θ_y and just multiply by 360° . We estimated them to be 37634 at $x_u=100$ mm, 33591 at 200 mm, 60765 at 300 mm, and 27090 at 350 mm, and 19613 at 400 mm. Since number of H^- in a 500 μsec macro pulse assuming a peak current of 20 mA and a duty factor of 0.4 (due to the chopping) is 2.5×10^{13} , we can calculate the beam loss fraction, namely observed H^+ to H^- ratio per m of 1.5×10^{-9} at $x_u=100$ mm, 1.3×10^{-9} at 200 mm, 2.4×10^{-9} at 300 mm, 1.1×10^{-9} at 350 mm, and 7.8×10^{-10} at 400 mm. Note these number are not corrected for detector efficiencies. These numbers should be compared to the estimated H^0/H^- ratio due to interaction of H^- with the remnant gas from the pressure inside the beam duct in the ACS section. Note that this H^0/H^- ratio should directly be compared to the observed H^+/H^- , since 100% of H^0 generated in the beam duct is converted to H^+ through the beam duct. Also the number of H^+ s directly generated in the interaction is 1 order smaller than the number of H^0 s. The estimated ratio is $\sim 2.7 \times 10^{-8}$ (1/m). The measured value is one order lower than this estimation. It may be explained by detector inefficiency and the fraction of H^0 to go out of the beam duct.

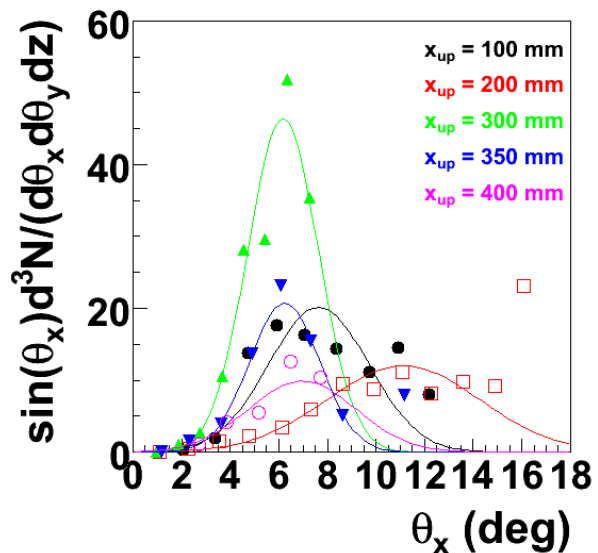


Figure 4: The beam loss spatial density ($\text{deg}^{-2}\text{m}^{-1}$) as a function of the horizontal track angle (deg).

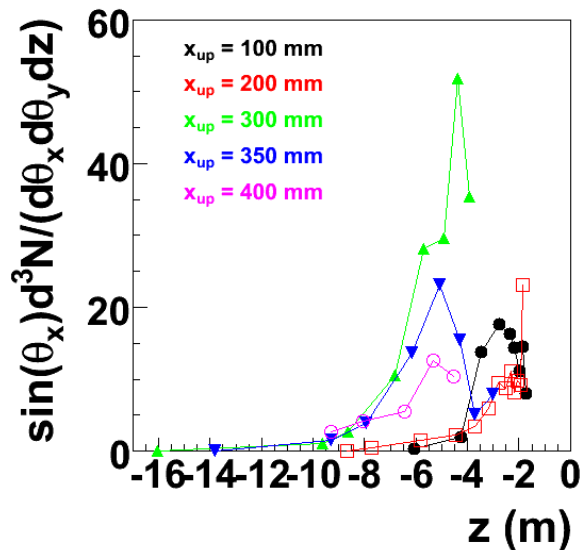


Figure 5: The beam loss spatial density ($\text{deg}^{-2}\text{m}^{-1}$) as a function of the source z-position (m).

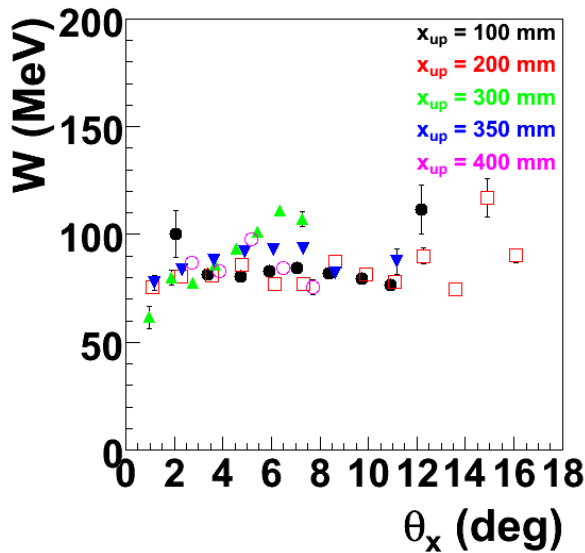


Figure 6: Energy (MeV) of the proton as a function of the horizontal track angle (deg).

The proton energy is plotted as a function of θ_x for different x_u settings in Fig. 6. The energy ranges 70-110 MeV. We expected from the simulation that the energy is lower at smaller beam angles due to energy loss in the 2 mm thick Ti beam duct, since a lower angle track penetrates effectively a thicker duct wall. This tendency is actually observed in the data at $\theta_x=0-6$ deg, and the strength of the tendency depends of x_u . Steep energy increases are observed at $x_u=300$ and 350 mm. On the other hand, a decrease of energy is observed from $\theta_x \geq 6$ deg, which we have not understood yet. As a result the maximum energy is observed at $\theta_x \sim 6$ deg.

CONCLUSIONS

In conclusion, we measured proton tracks due to beam loss at the ACS section in the J-PARC linac, with the scintillating fiber hodoscope system. We measured spatial distributions of proton tracks in the horizontal angle from 0 to 18 deg and upstream beam position from 2 to 16 m. From the measured number of protons, we estimated the uncorrected H^+/H^- ratio of $0.78-2.4 \times 10^{-9}$ per m. The average proton energy is measured to be 70-110 MeV, where maximum energy is observed around the horizontal angle around 6 degrees.

REFERENCES

- [1] H. Sako, *et al.*, "Beam Loss Particle Tracking in J-PARC Linac," 8th Annual Meeting of Particle Accelerator Society in Japan, Tsukuba, Japan, p. 501 (2011).
- [2] H. Sako, *et al.*, "Measurement of Beam Loss Tracks by Scintillating Fibers at J-PARC Linac," IPAC11, San Sebastian, Spain, 2011, p. 1251 (2011).

- [3] H. Sako, *et al.*, "Beam Loss Track Measurements by a Fast Trigger Scheme in J-PARC Linac," LINAC2012, Tel-Aviv, Israel, 2012, p. 663 (2012).

- [4] H. Sako, *et al.*, "Status of Beam Loss Spatial Distribution Measurements at J-PARC Linac", IPAC13, Shanghai, 2013, p. 524 (2013)